



Rapid and quantitative detection of multiple antibodies against SARS-CoV-2 mutant proteins by photo-immobilized microarray

Jun Akimoto^{1,2} · Hiroharu Kashiwagi¹ · Nobuhiro Morishima^{2,3} · Sei Obuse^{1,2} · Takashi Isoshima³ · Takahiro Kageyama⁴ · Hiroshi Nakajima⁴ · Yoshihiro Ito^{1,2,3}

Received: 3 June 2022 / Accepted: 30 June 2022 / Published online: 2 August 2022
© The Author(s), under exclusive licence to The Japan Society for Analytical Chemistry 2022

Abstract

A rapid automatic quantitative diagnostic system for multiple SARS-CoV-2 mutant protein-specific antibodies was developed using a microarray with photoreactive polymers. Two types of photoreactive polymers, phenylazide and polyoxyethylene, were prepared. The polymers were coated on a plastic plate. Aqueous solutions of mutant virus proteins were microspotted on the coated plate and immobilized by photoirradiation. Virus-specific IgG in the serum or blood was automatically assayed using an instrument that we developed for pipetting, reagent stirring, and washing. The results highly correlated with those of the conventional enzyme-linked immunoassay or immunochromatography. This system was successfully used to test the sera or blood from the patients recovered from the infection and the vaccinated individuals. The recovered individuals had antibodies against the nucleoprotein, in contrast to the vaccinated individuals. The amount of antibodies produced decreased with an increase in virus mutation. Blood collected from the fingertip (5 μ L) and a test period of 8 min were sufficient conditions for conducting multiple antibody assays. We believe that our system would facilitate rapid and quantitative automatic assays and aid in the diagnosis of various viral infectious diseases and assessment of the immune status for clinical applications.

Keywords COVID-19 · Microarray · Antibody detection · Blood test

Introduction

SARS-CoV-2 (severe acute respiratory syndrome coronavirus 2) has infected over a hundred million people and caused COVID-19 (Coronavirus disease 2019). It has led to over 6 million deaths worldwide till May 2022. In efforts to overcome the pandemic, various COVID-19 vaccines

were developed and are now available. However, as various mutants of SARS-CoV-2 have been emerging at intermittent intervals, it is important to understand the formation and function of virus-specific antibodies to produce more effective vaccines and to carry out scientific investigations to prepare for the future [1].

Various kits have been developed to detect SARS-CoV-2 antibodies. The use of these kits is guided by emergency use authorization (EAU) guidelines or has to be approved by the Food and Drug Administration (FDA). So far, only one test has received an EAU nod to be used as a quantitative assay. All other currently authorized tests are qualitative or semi-quantitative [2]. Antibody-testing technologies are mainly categorized into (a) single-use lateral flow tests (immunochromatography), where the presence of antibodies is demonstrated by a color change on a paper strip, and (b) laboratory-based immunoassays that allow the processing of many specimens simultaneously [3, 4]. In addition, some microarray systems have been developed for research purposes [5–16].

✉ Yoshihiro Ito
y-ito@riken.jp

¹ Emergent Bioengineering Materials Research Team, RIKEN Center for Emergent Matter Science, 2-1 Hirosawa, Wako-shi, Saitama 351-0198, Japan

² R-NanoBio Co., Ltd., Wako-RIKEN Incubation Plaza, 3-13 Minami, Wako-shi, Saitama 351-0104, Japan

³ Nano Medical Engineering Laboratory, RIKEN Cluster for Pioneering Research, 2-1 Hirosawa, Wako-shi, Saitama 351-0198, Japan

⁴ Department of Allergy and Clinical Immunology, Graduate School of Medicine, Chiba University, 1-8-1 Inohana, Chiba City, Chiba 260-8670, Japan

In our previous work, we developed a photoimmobilization microarray [17–26]. One of our systems, “DropScreen™” (Nippon Chemiphar, Tokyo, Japan), can also be used to launch an allergen microarray for clinical detection of IgE antibodies. It is available as part of health insurance coverage in Japan. We partially extended DropScreen for detecting antibodies against SARS-CoV-2 proteins [27]. The photoimmobilization methods can covalently immobilize various organic substances without any specific functional groups and with random orientation of antigens to expose various sites of immobilized antigens for interactions with polyclonal antibodies. Hence, photocrosslinking immobilization is more appropriate for the detection of antibodies in the serum or blood.

We previously reported a photo-immobilized microarray assay for SARS-CoV-2 antibodies [27]. Here, we use the photoimmobilization method employing two types of photoreactive polymers for quantitative and rapid detection of IgG against SARS-CoV-2 proteins of mutants using blood directly sampled from the fingertip. We then compare the developed method with the conventional enzyme-linked immunosorbent assay (ELISA) and immunochromatography assay (Fig. 1).

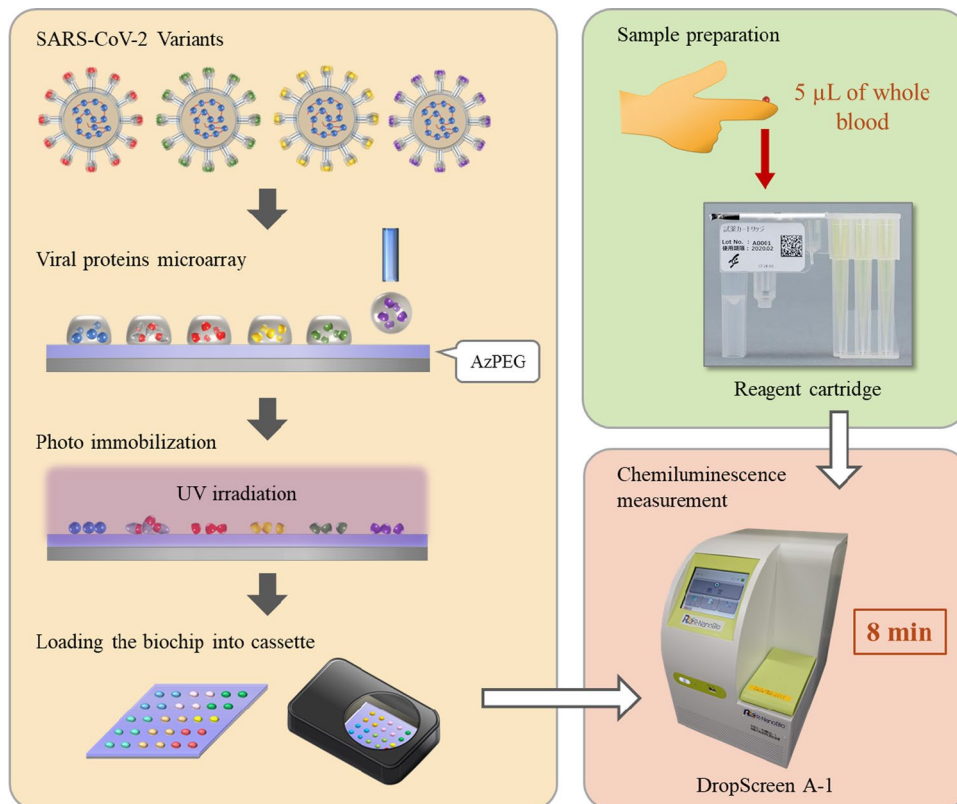
Materials and methods

Reagents and sera

Viral proteins are shown in Figure S1. SARS-CoV-2 proteins, including nucleocapsid protein, S1 protein, S2 protein, and spike protein RBDs (receptor-binding domain), were purchased from AcroBiosystems (Newark, DE, USA). The abbreviations of the purchased proteins and their sequences are listed in Table S1 and Figure S2, respectively.

Tween 20 (Sigma-Aldrich, St. Louis, MO, USA) and 2-amino-2-hydroxymethyl-propane-1,3-diol (Tris)-buffered saline (Takara Bio, Shiga, Japan) were mixed in water to obtain a buffer solution (TBST). Rabbit anti-SARS-CoV-2 antibodies used for control experiments were the same as previously reported [27]. Rabbit anti-nucleocapsid antibodies and anti-spike/RBD antibodies were diluted to 5000 and 500 times, respectively, while anti-rabbit IgG antibodies were diluted 12,000 fold. Normal human IgG was purchased from FUJIFILM Wako Pure Chemical (Osaka, Japan). Horseradish peroxidase (HRP)-conjugated goat anti-human IgG was also the same as previously reported [27]. For human sera and whole-blood measurements, 3000- and

Fig. 1 Schematic illustration of the microarray system



12,000-time dilutions of anti-human IgG antibodies were used to conduct the microarray assay for 8 and 30 min, respectively.

Human sera collected from COVID-19 recovered donors were the same as those used previously [27]. Vaccinated human sera and blood samples were collected from volunteers at Chiba University and RIKEN, respectively. The Chiba University Ethics Committee approved the procedures for sample collection and analyses on February 24, 2021 (No. HS202101-03) and April 21, 2021 (No. HS202104-01), respectively, while the RIKEN Ethics Committee approved them on October 7, 2021 (Wako3 2021-30) and February 7, 2022 (Wako3 2021-30(2)), respectively.

Preparation of photoreactive PEG

We used the photoimmobilization method using two types of photoreactive polymers for the detection of IgG against the SARS-CoV-2 protein. As shown in Figure S3, the polymers contained phenylazide groups and poly(ethylene oxide) in their side chains or main chain. The phenylazide-containing polymer was prepared as previously reported [27]. 4-Azidophenylmethacrylamide was synthesized and copolymerized with poly(ethylene glycol) methacrylate in the presence of 2,2'-azobisisobutyronitrile in ethanol for 18 h at 60 °C. The product was evaporated to remove ethanol and precipitated with ether to purify the product. This copolymer is referred to as AzPEG-1.

The poly(ethylene oxide)-containing polymer was also prepared as previously reported [28]. 4-(Glycidyloxy-methyl)azidobenzene was prepared from epichlorohydrin and 4-(hydroxymethyl)azidobenzene. The prepared 4-(glycidyloxy-methyl)azidobenzene was mixed with $[\text{MePPh}_3]^+\text{Br}^-$ under vacuum at 25 °C for 18 h. A solution of ethylene oxide and $i\text{-Bu}_3\text{Al}$ was added at -30 °C under argon, and the solution was stirred at 25 °C in the dark for 18 h. The solvent was then removed after the addition of methanol. The crude compound was dissolved in acetone and the precipitate was collected by filtration. The solution was precipitated using hexane and the precipitate was collected and dried under vacuum. The obtained polymer, poly(4-azidobenzyl glycidyl ether-*co*-ethylene oxide), was referred to as AzPEG-2(*x*). The number averaged molecular weight (M_n) of the polymers was determined by gel permeation chromatography (GPC) using a GPC system (JASCO, Tokyo, Japan) with two columns (SB803HQ and SB804HQ, Shodex, Tokyo, Japan) at 40 °C. The eluent was

DMF containing 10 mM of LiBr. The flow rate was 1.0 mL/min. Data were calibrated by PEG standards.

Photoimmobilization of proteins

The photoreactive polymer solution was spin-coated onto a plastic plate (Nippon Chemiphar) using a spin coater (Mikasa, Tokyo, Japan). The purchased solutions of SARS-CoV-2 proteins were diluted with phosphate-buffered saline (PBS). The protein solutions (60 µg/mL, 50 nL) were microspotted onto the coated plate using a microarrayer (Microjet, Nagano, Japan) and then allowed to dry. The microarrayed plate was photo-irradiated using a CL-1000 ultraviolet crosslinker (Analytik Jena, Jena, Germany) for 10 min. The antigen-immobilized plates were stored at 4 °C until further use.

Microarray assay

The automatic assay machine using the photo-immobilized biochip was developed by Nippon Chemiphar and Ueda Japan Radio (Nagano, Japan). The assay method was the same as previously reported [27]. Microarray plates immobilized with different virus proteins were incubated with a diluted solution of the serum or blood with shaking to complete the primary reaction between the immobilized virus proteins and antibodies. After the plate was washed in TBST, HRP-conjugated anti-human IgG antibodies were added to the microarray plate and incubated again with shaking to conduct the secondary reaction. This washing procedure was repeated to remove nonadsorbed detection antibodies. Finally, the Lumigen ECL Ultra (TMA-6) chemiluminescence substrate (Lumigen, Southfield, MI, USA) or Luminata™ Forte chemiluminescence substrate (Millipore-Sigma, Burlington, MA, USA) was added to the microarray plates and incubated further for imaging.

The measured chemiluminescence spots from each protein were partitioned into a grid pattern, and the luminescence intensity was analyzed by SpotSolverRK software (Ueda Japan Radio). Background luminescence intensity was measured by averaging the luminescence intensity value at the four corners of the grid on each protein spot.

Conventional ELISA and immunochromatography

Conventional ELISA was performed using two methods. Elecsys® Anti-SARS-CoV-2S on a Cobas 8000 e801 module (Roche Diagnostics, Rotkreuz, Switzerland) was used. This

Table 1 Composition of prepared photoreactive polymers

Sample	Monomer	Feed content of phenylazide (mol%)	Content of phenylazide in polymer (mol%)	Solvent	M_n^a	M_w/M_n^a
AzPEG-1	4-azidophenylmethacrylamide/poly(ethylene glycol) methacrylate	10	5.7	Ethanol	22,000	4.92
AzPEG-2 (2.5)	4-(glycidylloxymethyl)azidobenzene/ethylene oxide	2.5	1.3	Water	4500	1.72
AzPEG-2 (5)		5	3.1	Water	4600	1.40
AzPEG-2(10)		10	8.4	Ethanol	5400	1.99
AzPEG-2 (15)		15	13.5	Acetone	3000	1.77
AzPEG-2 (20)		20	17.8	Acetone	7000	3.17
AzPEG-2 (30)		30	30.3	Acetone	7400	1.55
AzPEG-2 (40)		40	42.3	Acetone	9100	1.56

^aDetermined by gel permeation chromatography

system allows quantitative detection of antibodies, predominantly IgG, targeting the SARS-CoV-2 spike protein receptor-binding domain. Samples with a titer > 250 U/mL were diluted 10 times until the titer reached ≤ 250 U/mL, according to the manufacturer's protocol. SARS-CoV-2 IgG II Quant Antibodies (Abbott Laboratories, Chicago, IL, USA) were used by Hyogo Clinical Laboratory (Hyogo, Japan).

Next, we performed immunochromatographic tests using a SARS-CoV-2 Rapid Antibody Test RUO (Roche Diagnostics), according to the manufacturer's protocol to detect IgG antibodies against SARS-CoV-2 in the human blood. Whole blood collected from the volunteers at RIKEN was diluted with PBS and used for the tests. The band color intensity was analyzed using ImageJ software.

Statistical analysis

Data are shown as the mean \pm standard deviation of three replicates unless specified otherwise. The graphs were plotted using Microsoft Excel.

Results and discussion

Photoreactive polymers and photoimmobilization

Table 1 shows the characteristics of the prepared photoreactive polymers. NMR spectroscopy was used to estimate the content of the phenylazide group. An increase in the phenylazide group content increased the hydrophobicity but decreased the solubility of the polymers in water. When the photoreactive polymers have over 5 mol% of phenylazide, they require ethanol or acetone in addition to water for their solubilization.

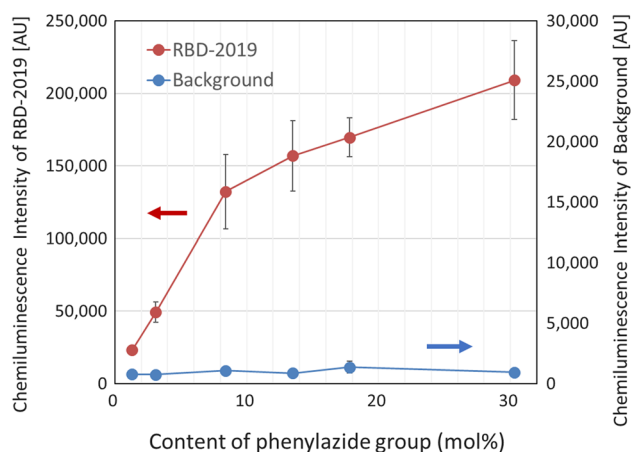


Fig. 2 Chemiluminescence intensity of rabbit anti-SARS-CoV-2 antibodies adsorbed on RBD-2019 immobilized with AzPEG-2(10)

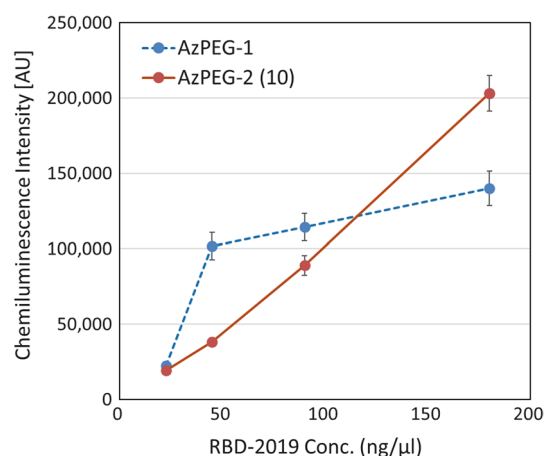


Fig. 3 Chemiluminescence intensity of rabbit anti-SARS-CoV-2 antibodies adsorbed on RBD-2019 immobilized with AzPEG-1 and AzPEG-2(10)

The prepared polymers were spin-coated, RBD-2019 was immobilized, and the chemical luminescence from the antibodies on the protein was measured (Fig. 2). When the phenylazide group content of the polymer was increased, the chemical luminescent signal also increased. As photoirradiation crosslinking reactions occur between virus protein and photoreactive PEG, photoreactive PEG and the plate surface, and within PEG chains in photoreactive PEG, the increase in the number of phenylazide groups improved the crosslinking efficiency. In addition, the background was very low and constant without using any blocking agent. A high S/N ratio was obtained even when no blocking agent was used.

Figure 3 shows the chemiluminescence of anti-RBD-2019 antibodies adsorbed on RBD-2019 immobilized with AzPEG-1 and AzPEG-2(10). AzPEG-2(10) increased the intensity more than AzPEG-1 does. In this study, the chemiluminescence intensity of AzPEG-2(10) was compared with that of AzPEG-1 that was our standard material to prepare the microarray system [25–27]. AzPEG-2(10) was used because its solubility and luminescence intensity were moderate compared with that of other AzPEG-2s with different compositions of the azidophenyl group.

AzPEG-2(10) increased the intensity more than AzPEG-1 does. At lower concentrations, the chemiluminescence intensity of RBD-2019-immobilized AzPEG-1 was higher than that of AzPEG-2. Because AzPEG-1 possessed a hydrophobic chain on its backbone, protein adsorption readily occurred on its surface. Meanwhile, the number of photoresponsive phenylazide groups on AzPEG-1 was lower than that on AzPEG2. Thus, the amount of RBD-2019 that can be immobilized on AzPEG-1 is limited. In contrast, the

hydrophilicity of AzPEG-2 is high. Thus, the adhesion of proteins decreases. However, AzPEG-2 possessed more phenylazide groups than AzPEG-1. As a result, the amount of immobilized RBD-2019 increased with increasing feed concentration of the protein, resulting in stronger luminescence.

Microarray assay

Some proteins of parts of SARS-CoV-2 were microarrayed and anti-RBD-2019 rabbit antibodies were detected, as shown in Fig. 4. When the photo-immobilized proteins were increased, the adsorbed antibodies also increased, which in turn increased the chemiluminescence. The highest intensity was observed for photo-immobilized RBD-2019 because an anti-RBD antibody was employed. However, it bound to S1 but not to S1 (NTD) because the former contains an RBD region, while the latter does not (Figure S1). The immobilized mutant RBDs had intermediate binding affinities to the antibody. Among the mutant RBDs, the omicron sequence had the lowest affinity for the antibody.

The correlation of the microarray method with other ELISA methods was also investigated using RBD-2019 (Fig. 5). Abbott and Roche assays did not show a very strong relationship. In contrast, our method highly correlated with the Abbott assay ($R^2=0.936$). Since the antibody detection by Abbott and Roche assays has different dynamic ranges, the correlation depends on the sampling time of blood [3].

Figure 6 shows the representative result of the antibodies produced by a recovered patient and a vaccinated person. The recovered patients had both anti-nucleoprotein and anti-S1 antibodies, whereas vaccinated persons had only anti-S1 antibodies. The affinity of antibodies produced by the human body by wild-type virus infection or vaccination for wild-type virus decreased from the wild RBD (RBD-2019) with the increase in mutant points.

Figure 7 shows antibody production before and after third vaccination. Although the amount of the antibodies produced varies person to person, the vaccination significantly induced antibody production. The vaccination also induced antibody production against omicron mutants. Since BS4 was from a person who recovered from the infection, the blood contained antibodies against both NP and RBD proteins.

Optimization of measurement conditions

In a previous study, we showed that the present method is more sensitive than immunochromatography (approximately 500-fold) [27]. However, our method took 30 min for the measurement. In this study, we reduced the measurement time. Table S2 shows operation times for the present method and the previous method. Because we used the clinically employed automatic measurement machine as hardware in

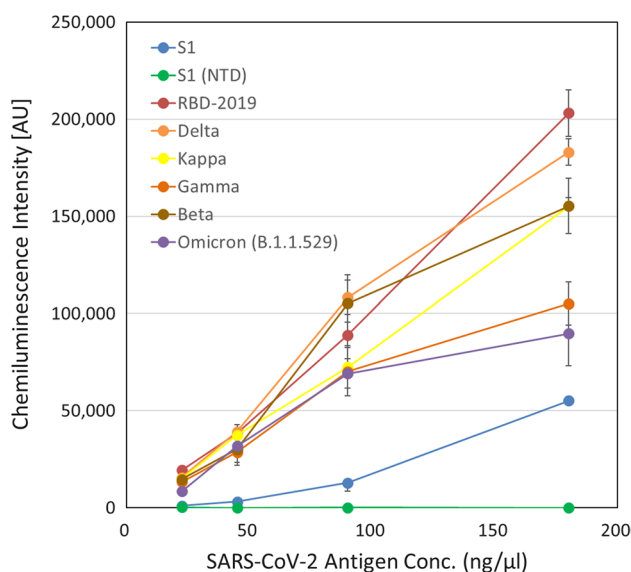


Fig. 4 Chemiluminescence intensity of rabbit anti-SARS-CoV-2 antibodies adsorbed on various SARS-CoV-2 virus proteins immobilized with AzPEG-2(10)

Fig. 5 Relationships between microarray assay on RBD-2019 immobilized with AzPEG-2(10), and ELISA using Abbott and Roche assays and 3000-time diluted human sera from volunteers at Chiba University. **a** Microarray vs. Abbott, **b** microarray vs. Roche, and **c** Abbott vs. Roche

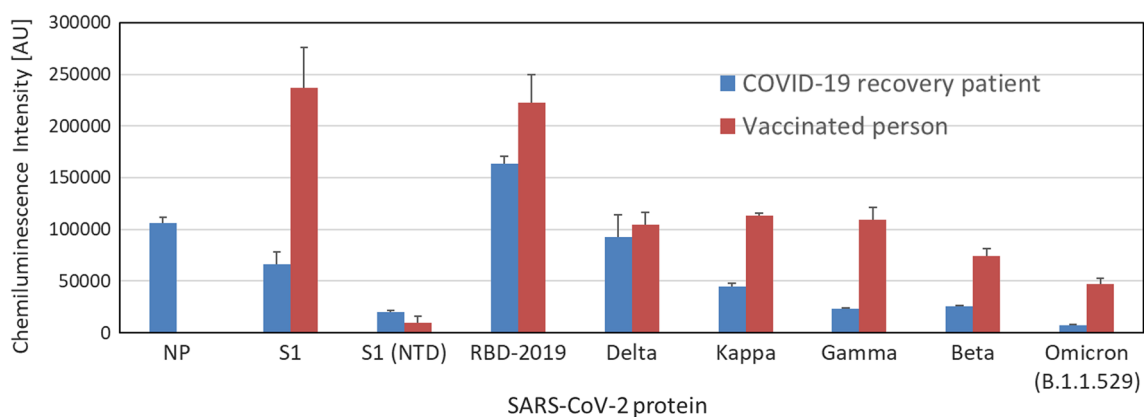
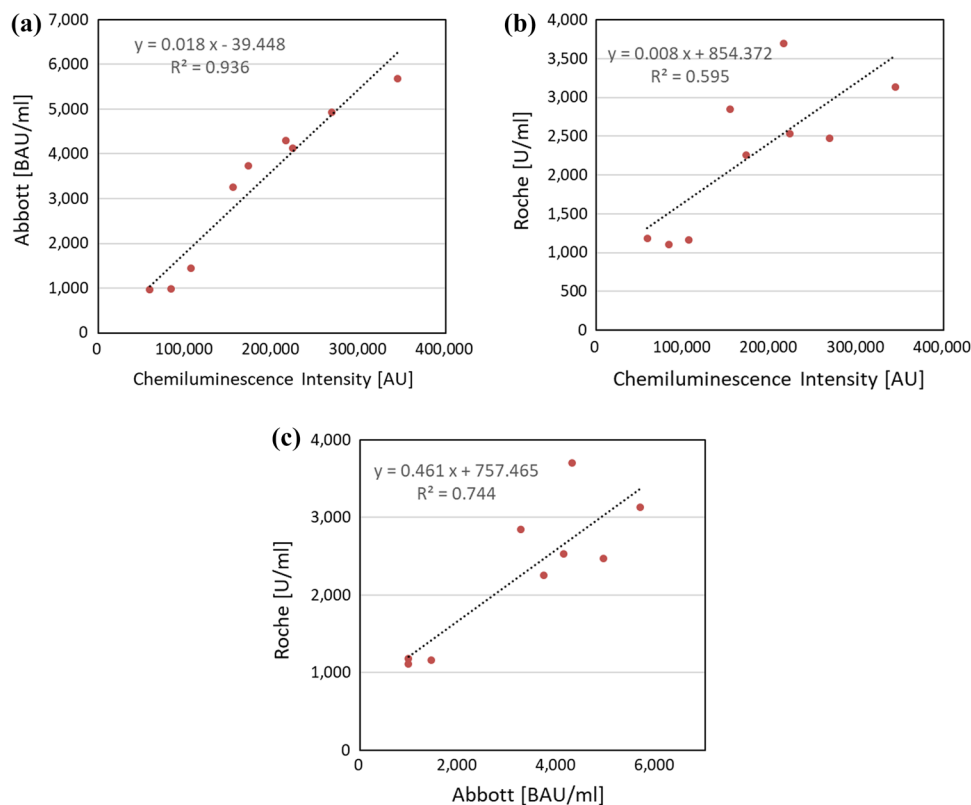


Fig. 6 Chemiluminescence intensity of serum antibodies adsorbed on photo-immobilized proteins by AzPEG-2(10). Serum dilution of the samples obtained from recovered and vaccinated volunteers was 1000 and 3000, respectively

this study, the total operation time included pipetting time, chip movement time, and washing time in addition to setting the parameter time of incubation for the reaction, washing, and imaging on DropScreen A-1 machine. The total measurement time was 8 min. Recently, microfluidic devices have been developed that can perform antibody detection using

only 16 μL of whole blood from the fingertip in just over 4 min [16].

In addition, to accelerate the development of automatic instruments, it is preferable to use the same reagent cartridge as that employed for allergy detection [27]. Because the previous dilution (3000) required too high a volume

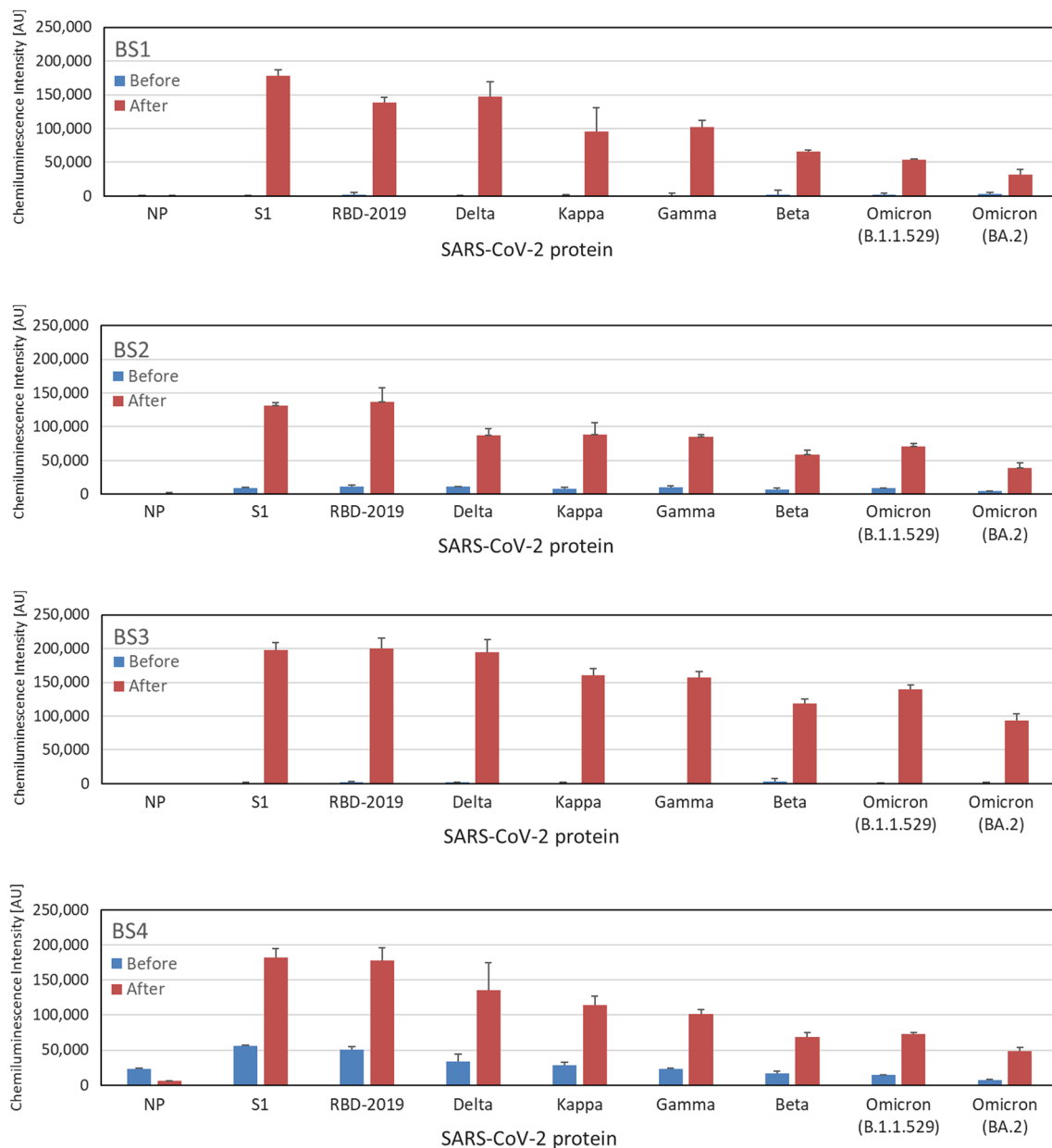


Fig. 7 Microarray assay of whole blood from an individual fingertip. The blood was sampled before and after third vaccination and the adsorbed antibodies on immobilized proteins with AzPEG-1. The blood was diluted to 50-fold

for the cartridge, the dilution was reduced to 50-fold. Figure 8 shows a comparison between the previous and present conditions. A high correlation was observed between the two conditions. The effect of reducing the volume of blood samples was also investigated. The results showed that 5 μ L of whole blood from the fingertip was sufficient for the measurement, although a slight decrease in

chemiluminescence was observed because of the difficulty in sampling (Fig. 9).

Finally, the chemiluminescence intensity of the microarray assay using RBD-2019 was compared with the quantification of the conventional immunochromatography assay (Fig. 10). The results showed a strong correlation between

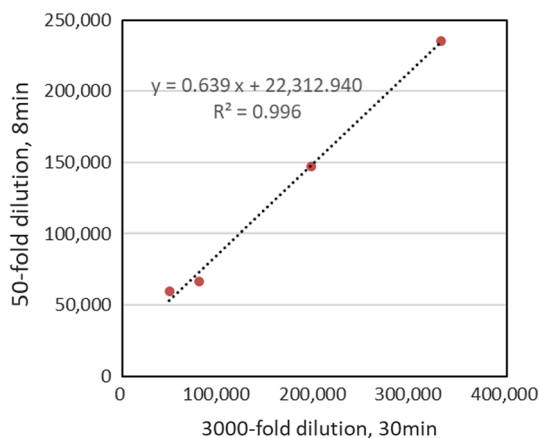


Fig. 8 Relationship of chemiluminescence intensity [AU] of antibodies adsorbed on RBD-2019 immobilized with AzPEG-I under different measurement times (30 and 8 min) and dilutions (3000- and 50-fold) of whole blood

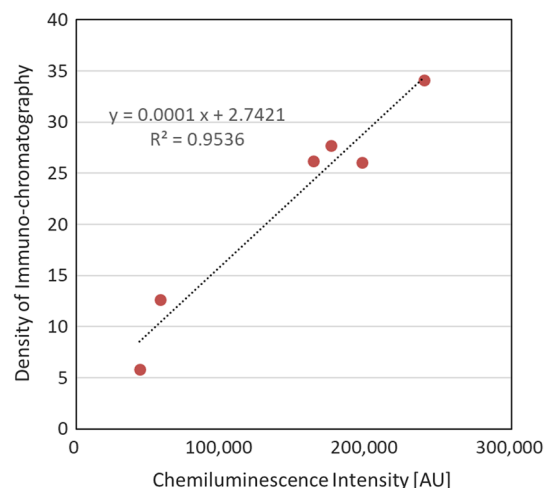


Fig. 10 Comparison of chemiluminescence intensity of antibodies for microarrayed RBD-2019 and for signal density of immunochromatograph using whole blood of fingertip (20 μ L). Whole-blood dilutions of microarray and immunochromatograph were 50-fold and 200-fold, respectively

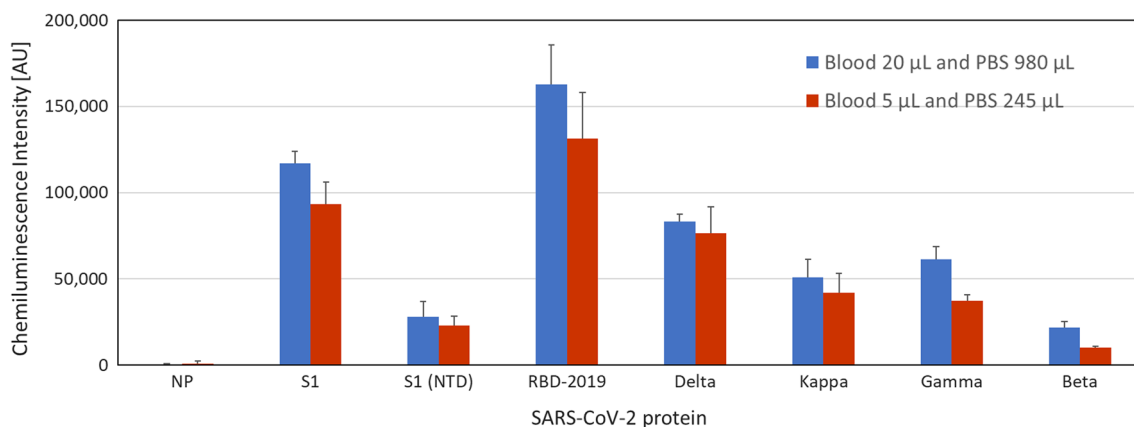


Fig. 9 Chemiluminescence intensity using 20 or 5 μ L of whole blood on various SARS-CoV-2 proteins under the same dilution (50-fold) for 8 min

them. The correlation coefficient for virus microarrays against immunochromatography was 0.95.

Conclusion

The assay can be performed much quicker than conventional immunochromatography with a higher sensitivity. Considering that the system is used clinically for the diagnosis of allergies, antibody detection can be performed at the level required for clinical diagnosis. As the present system is quantitative and requires less blood and a shorter measurement time than conventional ELISA or

immunochromatography, we believe it will be highly useful for various clinical applications.

Supplementary Information The online version contains supplementary material available at <https://doi.org/10.1007/s44211-022-00161-z>.

Acknowledgements We would like to thank Editage (<http://www.editage.com>) for English language editing.

Declarations

Conflict of interest The authors declare that they have no known competing financial interests or personal relationships that could have appeared to influence the work reported in this paper.

References

1. European Centre for Disease Prevention and Control, February 10, 2022 Considerations for the use of antibody tests for SARS CoV-2—first update (europa.eu)
2. Interim Guidelines for COVID-19 Antibody Testing by Centers for Diseases Control and Prevention January 24, 2022 Interim Guidelines for COVID-19 Antibody Testing | CDC
3. T. Perkmann, P. Mucher, N. Perkmann-Nagele, A. Radakovics, M. Repl, T. Koller, K.G. Schmetterer, J.W. Bigenzahn, F. Leitner, G. Jordakieva, O.F. Wagner, C.J. Binder, H. Haslacher, *Microbiol. Spectr.* **10**, e01402 (2022)
4. B. O’Kelly, R. McLaughlin, R. O’Doherty, H. Carroll, R. Murray, R. Dilworth, L. Corkery, A.G. Cotter, T. McGinty, E.G. Muldoon, W. Cullen, G. Avramovic, G. Sheehan, D. Sadlier, M. Higgins, P. O’Gorman, P. Doran, R. Inzitari, S. Holden, Y. O’Meara, S. Ennis, J.S. Lambert, *Front. Med.* **8**, 642318 (2021)
5. H. Wang, X. Wu, X. Zhang, X. Hou, T. Liang, D. Wang, F. Teng, J. Dai, H. Duan, S. Guo, Y. Li, X. Yu, *ACS Cent. Sci.* **6**, 2238 (2020)
6. P. Holenya, P.J. Lange, U. Reimer, W. Woltersdorf, T. Panterodt, M. Glas, M. Wasner, M. Eckey, M. Drosch, J.M. Hollidt, medRxiv 2020. <https://doi.org/10.1101/2020.11.24.20216663>
7. A. Musicò, R. Frigerio, A. Mussida, L. Barzon, A. Sinigaglia, S. Riccetti, F. Gobbi, C. Piubelli, G. Bergamaschi, M. Chiari, *Vaccines* **9**, 35 (2021)
8. D. Camerini, A.Z. Randall, K. Trappl-Kimmons, A. Oberai, C. Hung, J. Edgar, A. Shandling, V. Huynh, A.A. Teng, G. Hermanson, J.V. Pablo, M.M. Stumpf, S.N. Lester, J. Harcourt, A. Tamin, M. Rasheed, N.J. Thornburg, P.S. Satheshkumar, X. Liang, R.B. Kennedy, A. Yee, M. Townsend, J.J. Campo, *Microbiol. Spectr.* **9**, e01416 (2021)
9. J. Klüpfel, R.C. Koros, K. Dehne, M. Ungerer, S. Würstle, J. Mautner, M. Feuerherd, U. Protzer, O. Hayden, M. Elsner, M. Seidel, *Anal. Bioanal. Chem.* **413**, 5619 (2021)
10. J. Longworth, G. Dittmar, *STAR Prot.* **2**, 100815 (2021)
11. D. Ruano-Gallego, M. Garcia-Villadangos, M. Moreno-Paz, J. Gomez-Elvira, M. Postigo, M. Simon-Sacrist, H.T. Reyburn, C. Carolis, N. Rodrigo, Y.B. Codeseira, P. Rueda, S. Zuniga, L. Enjuanes, V. Parro, *Microb. Biotechnol.* **14**, 1228 (2021)
12. P.N. Hedde, T.J. Abram, A. Jain, R. Nakajima, R. Ramiro de Assis, T. Pearce, A. Jasinskas, M.N. Toosky, S. Khan, P.L. Felgner, E. Gratton, W. Zhao, *Lab Chip* **20**, 3302 (2020)
13. R.R. de Assis, A. Jain, R. Nakajima, A. Jasinskas, J. Felgner, J.M. Obiero, P.J. Norris, M. Stone, G. Simmons, A. Bagri, J. Irsch, M. Schreiber, A. Buser, A. Holbro, M. Battegay, P. Hosimer, C. Noesen, O. Adeniyai, S. Tai, F. Hong, D.K. Milton, H.D. Davies, P. Contestable, L.M. Corash, M.P. Busch, P.L. Felgner, S. Khan, *Nat. Commun.* **12**, 6 (2021)
14. J. Wang, Y. Yang, T. Liang, N. Yang, T. Li, C. Zheng, N. Ning, D. Luo, X. Yang, Z. He, G. Yang, B. Li, J. Gao, W. Yu, S. Gong, Y. Huang, J. Li, H. Wang, H. Zhang, T. Zhang, P. Li, Y. Li, J. Dai, X. Zhang, B. Li, X. Yu, H. Wang, *J. Adv. Res.* **37**, 209 (2022)
15. L. Mou, Y. Zhang, Y. Feng, H. Hong, Y. Xia, X. Jiang, *Anal. Chem.* **94**, 2510 (2022)
16. J. Klüpfel, S. PaBreiter, N. Weidlein, M. Knopp, M. Ungerer, U. Protzer, P. Knolle, O. Hayden, M. Elsner, M. Seidel, *Anal. Chem.* **94**, 2855 (2022)
17. Y. Ito, M. Nogawa, *Biomaterials* **24**, 3021 (2003)
18. Y. Ito, M. Nogawa, M. Takeda, T. Shibuya, *Biomaterials* **26**, 211 (2005)
19. K. Ohyama, K. Omura, Y. Ito, *Allergol. Int.* **54**, 627 (2005)
20. Y. Ito, T. Yamauchi, M. Uchikawa, Y. Ishikawa, *Biomaterials* **27**, 2502 (2006)
21. T. Matsudaira, S. Tsuzuki, A. Wada, A. Suwa, H. Kohsaka, M. Tomida, Y. Ito, *Biotechnol. Prog.* **24**, 1384 (2008)
22. S. Tsuzuki, A. Wada, Y. Ito, *Biotechnol. Bioeng.* **102**, 700 (2009)
23. Y. Ito, N. Moritsugu, T. Matsue, K. Mitsukoshi, H. Ayame, N. Okochi, H. Hattori, H. Tashiro, S. Sato, M. Ebisawa, *J. Biotechnol.* **161**, 414 (2012)
24. P.M. Sivakumar, N. Moritsugu, S. Obuse, T. Isoshima, H. Tashiro, Y. Ito, *PLoS ONE* **8**, e81726 (2013)
25. Y. Ito, H. Hasuda, M. Sakuragi, S. Tsuzuki, *Acta Biomater.* **3**, 1024 (2007)
26. Y. Ito, *Biotechnol. Prog.* **22**, 924 (2006)
27. H. Kashiwagi, N. Morishima, S. Obuse, T. Isoshima, J. Akimoto, Y. Ito, *Bull. Chem. Soc. Jpn.* **94**, 2435 (2021)
28. J. Akimoto, S.J. Park, S. Obuse, M. Kawamoto, M. Tamura, A. Nandakumar, E. Kobatake, Y. Ito, A.C.S. Appl, *Bio Mater.* **3**, 5941 (2020)